

Control of Complex Objects: Challenges of Linear Internal Dynamics

Won Joon Sohn¹, Rashida Nayeem¹, Ian Zuzarte², Neville Hogan³, Dagmar Sternad⁴

Abstract—Physical interaction with an object that has internal dynamics can be challenging, both for humans and robots. An example is carrying a cup of coffee, where the nonlinear dynamics between the cup and the liquid can be chaotic and unpredictable. This study examined how nonlinearity of an object’s dynamics contributed to the difficulty of a task and if linearization of the object dynamics facilitated performance. Human subjects did a task in a virtual set-up with a haptic interface using a robotic manipulandum. The task of transporting a cup of coffee was reduced to a 2D cart-and-pendulum model; subjects moved the cart and felt the dynamics of the pendulum representing sloshing coffee. Performance with the nonlinear system was compared to a linearized mass-spring version of the system. Subjects (n=16) executed continuous rhythmic, self-paced movements. In the linearized system subjects chose to move at frequencies close to the resonant frequencies and clearly avoided the anti-resonance frequency. In the nonlinear system subjects did not avoid the anti-resonance frequency. To evaluate performance, mutual information quantified predictability between the interaction force and the cup and object dynamics. Mutual information was lower in trials when the cup moved close to the anti-resonance frequency in both linear and nonlinear systems. The magnitudes of the interaction forces were higher in the linear system, especially at frequencies slightly below the anti-resonance. These results run counter to the expectation that linearization would simplify this task. These findings may be useful as design considerations for robot control and human-robot interaction: if humans interact with robots that exhibit complex dynamics in the frequency range of human actions, linearizing a nonlinear system may potentially disturb intuitive and low-effort cooperation.

I. INTRODUCTION

Interaction between humans and robots, traditionally confined to the industrial sector, is gradually entering the daily lives of all humans. There is a variety of ways that humans and robots can interact: Supportive interaction involves providing humans with tools or materials. An example of this is homecare robots where direct contact is minimized. Collaborative interactions include direct or indirect contact through a common medium that exchanges forces between the

*This work was supported by the following grants awarded to Dagmar Sternad: NIH R01-HD087089, NSF-CRCNS 1723998, NSF-NRI 1637854, NSF-M3X 1825942. Neville Hogan was supported in part by the Eric P. and Evelyn E. Newman Fund, NSF-NRI 1637824, NSF-CRCNS 1724135, NSF-M3X 1826097, NIH R01-HD087089.

¹Won Joon Sohn was with the Department of Electrical and Computer Engineering, Northeastern University, MA 02115 USA, phone: 617-373-5093; e-mail: wonjsohn@gmail.com

¹Rashida Nayeem is with the Department of Electrical and Computer Engineering, Northeastern University, MA 02115 USA, phone: 860-918-3342; e-mail: Nayeem.r@husky.neu.edu

human and robot [1, 2]. Recent advances in physical human-robot interaction also include soft robotics [3-5], such as control of passive elastic joints to improve performance [6], adaptive control methods to cope with uncertain inertia in robots with elastic joints [7], and adaptation of mechanical compliance during task execution [8]. It is noteworthy, though, that there is to date little understanding of how humans or robots interact with objects that have internal dynamics. This study examined human control of objects with passive internal dynamics.

A key requirement for successful physical interaction is that the actor, human or robot, can predict the object’s dynamics. A large body of research, using various methods, has investigated robot prediction of human behavior, such as recognition of human actions and gestures using Markov decision processes [9] and classification algorithms [10]. However, strategies for “hands-on” interaction with complex actuated objects have yet to receive the same attention. Before turning to actuated objects, this study examines control of objects with passive dynamics.

Due to the instantaneous nature of interaction forces when manipulating an underactuated object, predictability of the object’s dynamics is paramount. This is especially the case for complex dynamics, where nonlinearities may lead to chaotic behavior, which is essentially unpredictable. Previous research by our group examined human control of a ‘cup of coffee’, where the sloshing coffee creates complex interaction forces between hand and cup [11-13]. Using a simplified model of the real cup of coffee, a 2D cup with a ball sliding inside, previous research of our group reported evidence that humans increased the predictability of a complex underactuated object by exploiting the resonance frequencies of the system [14, 15]. These studies operationalized predictability by mutual information which quantified the mutual dependence between the hand and object dynamics. Results from these experiments showed that predictability was prioritized over low interaction forces. Three complementary studies operationalized predictability in terms of dynamic stability, using contraction

²Ian Zuzarte is with the Department of Bioengineering, Northeastern University, MA 02115 USA; e-mail: zuzarte.i@husky.neu.edu

³Neville Hogan is with the Department of Mechanical Engineering and Brain and Cognitive Sciences, Massachusetts Institute of Technology, Cambridge, MA 02139; e-mail: neville@mit.edu

⁴Dagmar Sternad is with the Department of Biology, Electrical and Computer Engineering, and Physics, Northeastern University, Boston, MA 02115; e-mail: d.sternad@northeastern.edu

analysis [16-18]. Stability ensures predictability as small errors are rejected and the system returns to its stable state. Experimental results supported the hypothesis; human subjects indeed increased the contraction of their trajectories with practice.

Following that previous research, this study focused on the effect of nonlinearity on predictability in human interactive strategies. Typically, linear object dynamics are more predictable as they eliminate the potential for chaotic behavior. Hence, interaction with a linear system should be easier.

To test this hypothesis, this study again used the task of transporting a ‘cup of coffee’. This everyday task exemplified the challenge of controlling a nonlinear system with its complex and potentially chaotic interactive dynamics, not only between the hand and the cup, but also between the cup and the liquid. The experimental system simplified the ‘sloshing coffee’ to the well-known cart-and-pendulum system that included nonlinear pendulum dynamics. To assess the impact of this nonlinearity, the dynamics of the cart-and-pendulum were linearized. The experiment compared how human performance changed when presented with linear and nonlinear object dynamics. Both the nonlinear and linearized systems were implemented in a virtual environment in which the subjects interacted with visual and haptic interfaces. The hypothesis was that the linearized object dynamics had more predictable behavior that would make interaction more predictable and rendered the manipulation less effortful.

II. EXPERIMENTAL APPARATUS

A. Mechanical model of the task

Transporting the cart-and-pendulum was presented on a projection screen as a 2D semicircular arc (cup) containing a freely-moving ball (Fig.1A,B). Assuming that the ball did not roll, but only slid without friction along the arc, the system was mathematically identical to the well-studied cart-and-pendulum system (Fig.1C). The motion of the cup was limited to a horizontal direction, similar to previous implementations [11, 13-15]. Although the system was markedly simpler than a real 3D cup with sloshing coffee, it preserved two important dynamical properties: it was underactuated and nonlinear.

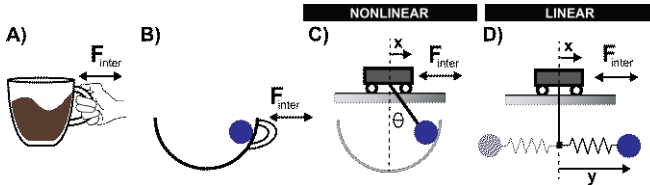


Figure 1. Real task and the two models of the task. **A)** Cup of coffee interacting with the hand. **B)** Simplified 2D cup with a ball representing the sloshing coffee. **C)** Nonlinear cart-and-pendulum model. **D)** Equivalent linearized cart-and-pendulum model with the ball limited to horizontal motion.

B. Nonlinear cart-and-pendulum system

The motion of the cup was simulated as a cart with mass M and a simple pendulum with point mass m (the ball) attached to a massless rod of length l (Fig.1C). The equations of motion were:

$$(m+M)\ddot{x} = F_{Ball} + F_{Inter} \quad (1)$$

$$= ml(\ddot{\theta} \cos \theta - \dot{\theta}^2 \sin \theta) + F_{Inter} \quad (2)$$

$$l\ddot{\theta} = \ddot{x} \cos \theta - g \sin \theta \quad (2)$$

where θ , $\dot{\theta}$ and $\ddot{\theta}$ represented the ball kinematics (angular position, velocity and acceleration): x , \dot{x} , and \ddot{x} denoted the cup position, velocity and acceleration, respectively. F_{Inter} was the interaction force applied to the cup by the hand; and g was the gravitational acceleration. There were two distinct forces that determined the motion of the cup: those applied by the user onto the cup F_{Inter} and the reaction forces generated by the motion of the ball F_{Ball} . In the experimental implementation, the values of M , m and l were set to 2.4kg, 0.6kg and 0.45m, respectively. The angle of the ball θ was defined as 0deg at the downward vertical position and positive values described the counter-clockwise direction.

C. Linearization of the system

The system dynamics were linearized using the small angle approximation around the downward vertical position of the pendulum. The linear behavior of the ball was enforced over the full range of ball motion. As a result, the ball force was generated by a linear spring; ball position was relabeled to y (Fig.1D). In the linear case the force of the ball could grow without bound. The ball force was multiplied by a scaling factor c to ensure that the magnitude of the ball force was not too large; in the experiment, c was set to 0.10. The resultant equations of motion for the linearized dynamic system of the cup-and-ball were:

$$(m+M)\ddot{x} = cm\ddot{y} + F_{Inter} \quad (3)$$

$$\ddot{y} = \ddot{x} - \frac{g}{l}y \quad (4)$$

D. Experimental apparatus and protocol

Sixteen healthy subjects (24.2 ± 2.1 yrs, 5 male) were seated on a chair in front of a back-projection screen positioned 2.0m in front of them; they interacted with the virtual environment via a robotic manipulandum (HapticMaster®, Motekforce, Amsterdam, NL). Details of the robot are reported in [19]. Using their dominant hand, subjects grasped a small knob at the end of the HapticMaster robot with a three-finger grip to interact with the simulated cup-and-ball system (Fig.2). The cup was represented by a semicircular arc with a radius equal to the pendulum length l ; the arc was drawn below the ball so that the ball appeared to roll in the cup. The ball could not escape from the cup and would continue swinging around the cup if the pendular rotation exceeded 90deg. Both the linear and nonlinear system showed the same ‘cup’ display. Two green rectangular targets were displayed on the screen as amplitude targets. The on-screen minimum distance between the centers of each target was 66.8cm, but the target width provided a large tolerance, allowing a maximum movement amplitude of 82.5cm. This permitted subjects to freely move at their preferred amplitude and frequency. The actual physical distance traversed with the robot manipulandum between the target centers was only 16.7cm due to the screen-scaling factor of 4.

Participants applied force on the knob of the robotic arm F_{inter} to control the 1D horizontal position of the virtual cup x . Participants sensed the ball's reaction force F_{ball} via the haptic force feedback from the robotic manipulandum [20]. A custom-written C++ program based on the HapticAPI (Moog FCS Control Systems) computed the ball kinematics and the virtual display as well as the feedback force.

III. EXPERIMENTAL PROTOCOL

Subjects were instructed to move the cup back and forth rhythmically and as comfortably as possible between the two green target boxes; they were encouraged to freely choose their amplitude (Fig.2). In the self-paced (SP) trials, subjects were also free to choose their frequency of oscillations.

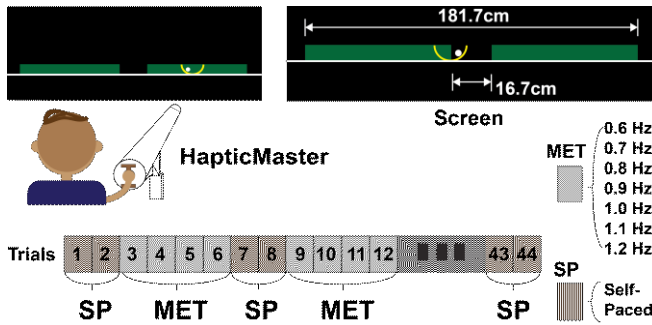


Figure 2. Experimental apparatus and protocol. The participant used the HapticMaster robot to interact with the virtual cup-and-ball system. The position of the end-effector of the robot was mapped to the position of the cup.

These 16 self-paced trials were interleaved with metronome-paced (MET) trials set to one of seven different frequencies: 0.6, 0.7, 0.8, 0.9, 1, 1.1 and 1.2Hz (Fig.2). The purpose of these paced trials was to expose subjects to a wide range of frequencies and discourage them from continuing at their initial choice of frequency. Subjects performed 2 experimental sessions on 2 consecutive days. On one day they manipulated the nonlinear system, on the other day the linearized system; the order of the two conditions was counterbalanced across subjects. Each session comprised 2 self-paced trials followed by 4 metronome-paced trials at 2 randomly selected frequencies, again succeeded by 2 self-paced trials. This sequence of un-paced and paced trials was repeated until every MET frequency was presented 4 times; this summed to a total of 44 trials, each lasting 35s. In each trial the cup started at the center of the left target box with the ball positioned at the bottom of the cup. This paper presents analysis of only the self-paced trials.

A. Estimation of mechanical hand impedance

The interactive dynamics that coupled the hand and object were approximated by a stiffness k in parallel with a damping b both set to constant value as shown in Fig.3. This impedance system served to minimize the errors between the actual cup trajectory and the cup trajectory desired by the human. Humans are imperfect actuators and due to the internal dynamics of the system their cup trajectories were not always accurate. The impedance served as a simple proportional-

derivative controller to minimize the human error. The trajectories were simulated by forward dynamics with the force F_{inter} of the hand applying force onto the system. In the following equation, x is the actual cup position, x_{des} is the desired cup position, \dot{x} is the actual cup velocity, and \dot{x}_{des} is the desired cup velocity.

$$F_{inter} = -k(x - x_{des}) - b(\dot{x} - \dot{x}_{des}) \quad (5)$$

Since the parameters for hand impedance k and b could not be measured directly, their values were estimated by an optimization procedure. This procedure identified the best fit between the simulated and experimental trajectories (see [14]). To determine the impedance parameters, an optimization procedure was conducted that tested k and b values in the ranges: $50 < k < 350$ N/m, step size: 2 N/m, $3 < b < 53$ N·s/m, step size: 1 N·s/m. The simulations were performed for all combinations of k and b . Each simulation run matched the frequency of the respective trial. For each trial, those k and b values were selected that yielded the smallest root mean square errors rms of the 4 state variables $x(t)$, $\dot{x}(t)$, $\theta(t)$, $\dot{\theta}(t)$:

$$C = \frac{1}{4} \left[\frac{rms(x^e - x^s)}{\|x^e\|_\infty} + \frac{rms(\dot{x}^e - \dot{x}^s)}{\|\dot{x}^e\|_\infty} + \frac{rms(\theta^e - \theta^s)}{\|\theta^e\|_\infty} + \frac{rms(\dot{\theta}^e - \dot{\theta}^s)}{\|\dot{\theta}^e\|_\infty} \right] \quad (6)$$

where superscript s and e denotes simulation and experiment, respectively. The two impedance parameters were obtained for each individual trial and then averaged across trials. The average parameter values were: $k=92.9 \pm 33.8$ N/m, $b=38.8 \pm 21.4$ N·s/m, which were consistent with values from the literature [21, 22]. Using these estimated parameters in the coupled model (Fig.3), a frequency response analysis of the linearized system could be conducted.

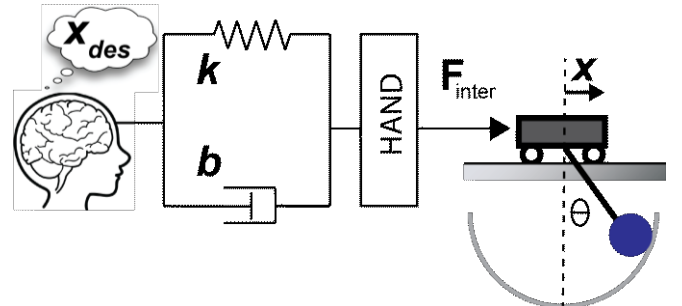


Figure 3. Control model of the cart-and-pendulum system with desired trajectory and hand impedance.

The internal degree of freedom of the cup-and-ball interacted with the hand impedance to produce two resonant frequencies. Due to bidirectional interactions, both resonant frequencies were determined by the subjects' interactive dynamics as well as the object dynamics. These two resonances were separated by an anti-resonance, a dynamic zero. For both the linear and nonlinear system, the anti-resonance was independent of subjects' interactive dynamics, determined by the natural behavior of the pendulum when the cart was stationary:

$$f_{zero} = \frac{1}{2\pi} \sqrt{g/l} = 0.74 \text{ Hz} \quad (7)$$

B. Data processing and analysis

The force applied by the subject and the position, velocity, and acceleration of the cup and ball were recorded at 120Hz for offline analysis. To eliminate transients only the last 25s of each trial were analyzed. All data processing and analysis was performed in MATLAB v.2017b and Simulink v.9.0 (The Mathworks, Natick, MA). The force data were smoothed using a second-order Savitzky-Golay FIR filter.

Each subject's behavior was characterized by three measures: 1) frequency of cup oscillation, 2) mutual information between interaction force and cup motion as a measure of predictability, 3) magnitude of interaction force between hand and cup to quantify exerted effort.

Movement frequency: Each trial's frequency was determined by finding the zero crossings of cup velocity \dot{x} , calculating the period of each cycle and its inverse, and averaging the values over the last 25s.

Mutual information: To quantify the predictability of the object dynamics mutual information MI , a measure of mutual dependence between two variables, was calculated between the cup movement and the interaction force $F_{inter}(t)$. The cup dynamics was represented by its phase $\varphi(t) = \arctan(\dot{x}/2f\pi x)$.

$$MI(\varphi, F_{inter}) = \iint p(\varphi, F_{inter}) \ln \left[\frac{p(\varphi, F_{inter})}{p(\varphi)p(F_{inter})} \right] d\varphi dF_{inter} \quad (8)$$

where p denotes the probability density functions for $\varphi(t)$ and $F_{inter}(t)$. The probability density functions were estimated by linear interpolation of nonlinear Gaussian smoothing kernels, using Silverman's method for finding the parameters [23].

Interaction force: The continuous interaction force was measured and the root mean square (RMSF) over the trial's time series was calculated:

$$RMSF = \frac{1}{T} \int_0^T F_{inter}^2(t) dt \quad (9)$$

where T was the 25s duration of the trial.

IV. RESULTS

A. Time series of kinematics

Fig.4 shows exemplary time series of ball kinematics and interaction forces at three different frequencies: 1) below anti-resonance, 2) near anti-resonance, and 3) above anti-resonance, for 15s each. For both linear and nonlinear systems, the cup and ball positions were in-phase at frequencies below the anti-resonance, and in anti-phase relation at frequencies above the anti-resonance. This was confirmed via forward simulations of the model. Near anti-resonance the ball and cup kinematics showed erratic behavior, reflecting the subjects' inability to achieve consistent movements due to unpredictable interaction forces.

There were no visible differences between the time-series in the linear and nonlinear trials, except near the anti-resonance frequency. There were also no visible differences in the chosen amplitudes of cup movements.

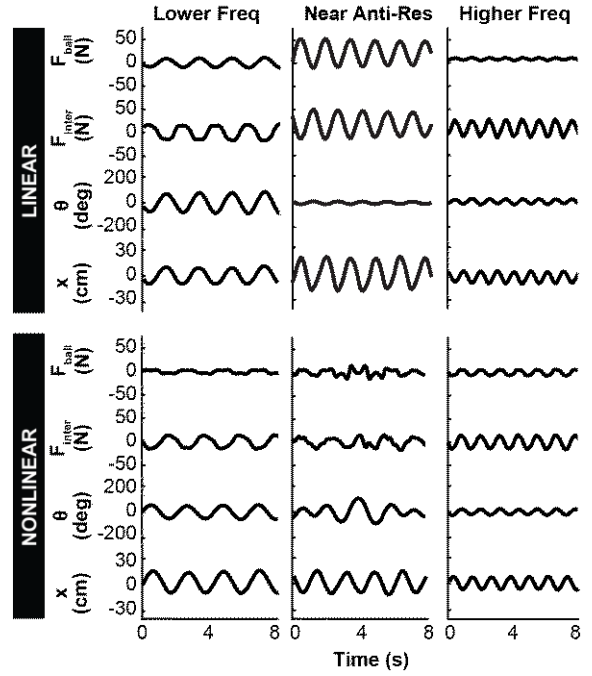


Figure 4. Exemplary time series data. Linear system with the cup frequency below, near, above anti-resonance. Nonlinear system with the cup frequency below, near, above anti-resonance. For the given parameters of the cup and ball system in the lower frequency strategy, the cup and ball position are in phase. For the high frequency strategy, the cup and ball position are in anti-phase. Near the anti-resonance the system exhibits quasi-chaotic behavior.

B. Histogram of chosen cup frequencies

The histograms in Fig.5 show the preferred frequencies of cup motions for the self-paced trials for all subjects; each count represents the mean frequency per trial (bin size=0.08 Hz). The visible bimodal distribution for the linear system indicates that subjects avoided frequencies around 0.74Hz, the anti-resonance frequency. In contrast, in the nonlinear system the preferred frequencies were distributed more evenly and did not show this 'dip'. The Hartigan's dip test, a statistical test for unimodality, confirms that the linear system was bimodally distributed ($D=0.0509$, $p=1.4e-4$), and the nonlinear system was not ($D=0.0329$, $p=0.0810$), where $p<0.05$ indicates significant bimodality. This suggests that the linear system presented more challenges for interactions as it appeared to discourage subjects from moving at frequencies close to the anti-resonance.

To interpret the frequency preferences of subjects in the linear system, a frequency response was calculated using the mean estimated impedance parameters ($k=92.9 \text{ N/m}$, $b=38.8 \text{ N}\cdot\text{s/m}$). The cup amplitude/input force was overlaid on the histogram (not to scale). The frequency response of the cup movement matched the frequency peaks in the histogram for the linear system, although the model peaks were not as

pronounced (Fig.5A,B). This analysis was not conducted for the nonlinear system as a more complex, amplitude-dependent response is observed.

C. Mutual information and predictability

Fig.6A shows the mutual information values for each trial plotted against its mean frequency for all 16 subjects. The pattern of mutual information across frequencies was similar for the linear and nonlinear systems, showing a marked decrease of MI at the anti-resonance frequency. However, in the nonlinear system there were a few trials with frequencies close to the anti-resonance. In contrast, in the linear system subjects completely avoided moving at the anti-resonance. Especially at frequencies slightly higher than 0.74Hz, the MI values were very low indicating that hand-object dynamics was more complex and less predictable. Note that these data do not support the hypothesis that the linear system provided the subject with more predictable dynamics.

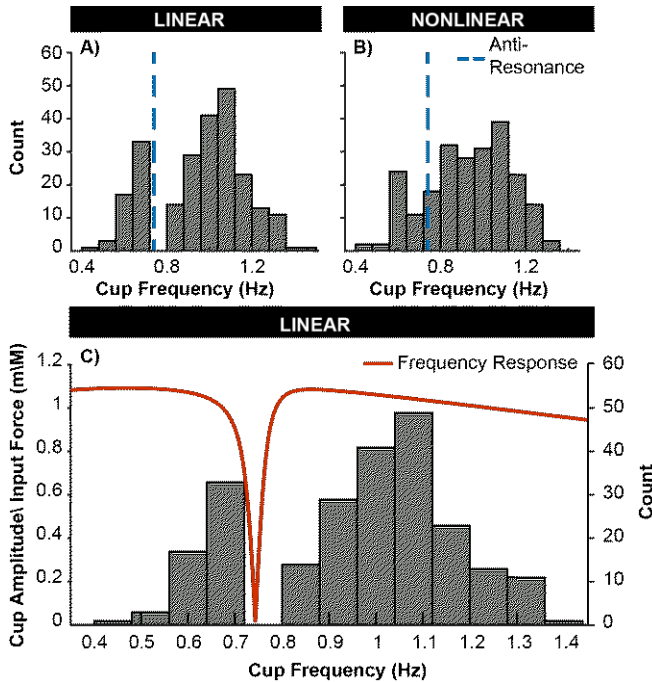


Figure 5. Histogram of chosen frequencies and the frequency response calculated from the model. **A)** Chosen cup frequencies in the linear system. **B)** Chosen cup frequencies in the nonlinear system. **C)** Histogram of the linear system with the frequency response from the coupled model (the hand impedance coupled to the cup and ball system).

D. Interaction force and effort

Fig.6B shows the root mean square of the continuous interaction force $RMSF$ as a measure of the exerted effort. The $RMSF$ value of each trial was plotted versus its mean frequency for all 16 subjects. In the linear system, $RMSF$ steeply increased from the lower frequency range to the anti-resonance at 0.74Hz. In contrast, in the nonlinear system, $RMSF$ did not show the same sensitivity to the frequency; it only gradually increased at the higher frequencies, independent of the anti-resonance. This pattern was counter to the expectation that subjects could lower their interaction forces in the linear system.

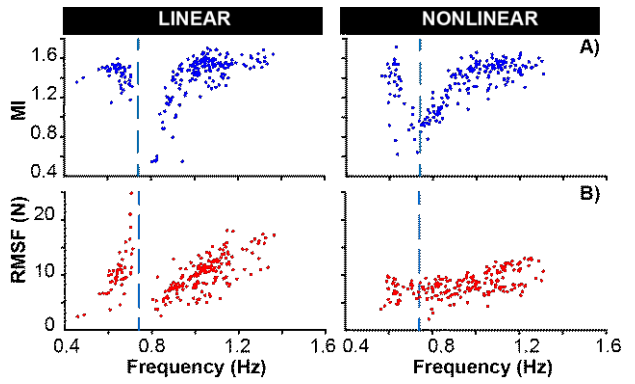


Figure 6. Mutual information and root mean square interaction force (RMSF) for all 16 subjects. **A)** Mutual information between the interaction force and object kinematics for the linear and nonlinear system, plotted across chosen frequencies. Each dot represents a trial. **B)** RMSF for the linear and nonlinear system across the chosen frequencies. The dotted vertical lines indicate the anti-resonance frequency.

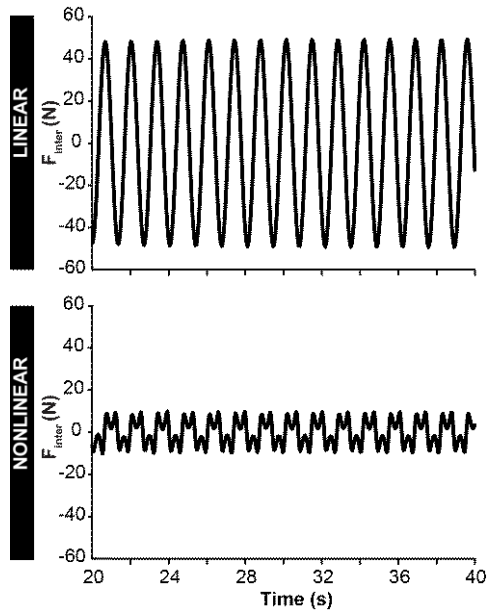


Figure 7. Zero dynamics force solution for the linear and nonlinear system both at 0.74 Hz. The time series starts 20s after the beginning of the trial to eliminate the initial transients.

E. Anti-resonance and zero dynamics

In both the linear and nonlinear cases at anti-resonance, reaction forces from the pendulum induce zero dynamics, a time-history of non-zero input force that yields zero cup motion. Why did the linear system seem to present more difficulties at the anti-resonance frequency? To address this question the two input force profiles that resulted in zero output motion of the cup were computed. Fig.7 shows that the zero-dynamics profile for the linear system was a simple sinusoidal function, whereas for the nonlinear system the input force had more than one frequency component. As the cup movements were instructed to be approximately sinusoidal, the zero-dynamics condition could be relatively easily met in the linear system, leading to a significant disruption or even cancelling of the intended movement.

Also, in the linear system the input that resulted in the zero-dynamics condition had much higher force values relative to the zero-dynamics condition in the nonlinear case. Therefore, subjects may have avoided the anti-resonance because F_{ball} at 0.74Hz transmitted relatively high forces onto the hand. In contrast, in the nonlinear system the zero-dynamics profile was easier to miss as it was less likely that subjects would follow the more complex profile for any length of time to experience the disruptive zero dynamics. With the task-instructed sinusoidal force subjects could be at, or close to this frequency without encountering the nulling effect.

V. DISCUSSION

This study examined strategies adopted by humans when manipulating objects with both linear and nonlinear internal dynamics. The hypothesis was that when humans manipulated objects with linear dynamics the interactions would be more predictable and less effortful. To test human behavior in these two cases the experimental instruction did not specify frequency or amplitude, but rather examined the range of preferred movements that humans adopted. Counter to the hypothesis, the interactions were more effortful in the linear system. Also contrary to prior belief, the linear system afforded only a restricted range of frequencies due to its disruptive zero dynamics and relatively high forces at the anti-resonance. Therefore, for human-robot cooperation, linear dynamics may not necessarily simplify interaction.

The frequencies that subjects adopted showed a clear bimodal distribution in the linearized system, while in the nonlinear system participants visited the whole range of frequencies, including the system's dynamic zero, or anti-resonance. This highlighted that the 'simple' dynamics of the linear system actually may have made the system more difficult to manipulate for the human participant. The zero-dynamics condition is an important consideration in the design and analysis of nonlinear control systems, e.g. in feedback linearization. The nonlinear system required a more complex interaction force to achieve its zero-dynamic state. Subsequently, subjects could move the cup at anti-resonance in the nonlinear system because they were unlikely to match the interaction force profile that would cause zero cup motion.

Note that a previous study on the same experimental paradigm reported a bimodal distribution of frequencies for the nonlinear system [14]. However, in the previous study the amplitude of cup movement was fixed, which limited the movement frequency choices above and below the anti-resonance frequency.

It is important to note that the two resonances were generated by the coupled system that included the impedance of the hand. Thus, the location of these resonant frequencies could be influenced by the subjects' movements and their chosen impedances. Note, however that anti-resonance is determined solely by the natural behavior of the pendulum. For the simulations reported here, the impedance values were obtained from an optimization procedure estimating the best

fit to the state variables of the system [14]. The frequency response was calculated for the mean impedance parameters. As the parameters tended to be different for the lower and higher frequencies, a better fit on the peaks of the histogram may be obtained if two different response functions were calculated for the lower and higher frequencies [14].

One corollary of the hypothesis about predictability was that the human interaction force would be less effortful when interacting with the linear model. The results did not support this expectation. In the nonlinear case, the ball force was limited by its periodic dependence on ball angle. The linearized model had no comparable limitation. The linearized spring forces were not bounded by the circular motion of the pendulum as in the nonlinear model.

In summary, the main expectations of this study were that linearity affords less effortful performance and easier prediction of the system dynamics. Counter to expectations, movements with the linearized system created relatively higher forces, especially at the anti-resonant frequency. Assessing predictability by mutual information, the metric showed that, contrary to prior assumptions, there were no clear differences between the linear and the nonlinear system except at anti-resonance. Simulations confirmed that for the linear system a simple sinusoidal input force at the anti-resonant frequency would cause the zero-dynamic state. As such a simple sinusoid coincided with the task-instructed movement, subjects avoided moving at the anti-resonant frequency.

VI. CONCLUSION

This study investigated the strategies that human participants adopted to interact with a non-rigid object with complex dynamics during a rhythmic manipulation task. Specifically, the study examined how the system's nonlinearity contributed to the challenge of controlling a complex object by contrasting the human's interaction with nonlinear and linear systems. Contrary to our hypothesis, linearized object dynamics were neither more predictable, nor less effortful to interact with. In the linear system the chosen cup movements clearly avoided the zero-dynamic frequency which restricted the range of interaction frequencies.

These results suggest that it may not always be necessary to linearize haptic feedback in human-robot interaction. Although enforcing linear behavior might be useful for certain controller designs, e.g. feedback linearization, this may potentially restrict interactive behavior, especially if dynamic zeros coincide with the frequency range of human actions. These results may inform the design of a range of robotic applications including assisted industrial manipulation, collaborative assembly, home assistance and rehabilitation.

REFERENCES

- [1] B. Siciliano and O. Khatib, "Springer Handbook of Robotics Preface to the Second Edition," *Springer Handbook of Robotics*, pp. Xvii-Xviii, 2016.
- [2] A. Ajoudani, A. M. Zanchettin, S. Ivaldi, A. Albu-Schäffer, K. Kosuge, and O. Khatib, "Progress and prospects of the human–robot collaboration," *Autonomous Robots*, vol. 42, no. 5, pp. 957-975, 2018.
- [3] S. Kim, C. Laschi, and B. Trimmer, "Soft Robotics: a Bioinspired Evolution in Robotics," *Trends in Biotechnology*, vol. 31, no. 5, pp. 23-30, May 2013.
- [4] N. S. Lu and D. H. Kim, "Flexible and Stretchable Electronics Paving the Way for Soft Robotics," *Soft Robotics*, vol. 1, no. 1, pp. 53-62, Mar 2014.
- [5] C. Majidi, "Soft Robotics: A Perspective-Current Trends and Prospects for the Future," *Soft Robotics*, vol. 1, no. 1, pp. 5-11, Mar 2014.
- [6] B. Siciliano and L. Villani, "An Inverse Kinematics Algorithm for Interaction Control of a Flexible Arm with a Compliant Surface," (in English), *Control Engineering Practice*, vol. 9, no. 2, pp. 191-198, Feb 2001.
- [7] M. W. Spong, "Adaptive-Control of Flexible Joint Manipulators," (in English), *Systems & Control Letters*, vol. 13, no. 1, pp. 15-21, Jul 1989.
- [8] N. Hogan, "Adaptive-Control of Mechanical Impedance by Coactivation of Antagonist Muscles," (in English), *IEEE Transactions on Automatic Control*, vol. 29, no. 8, pp. 681-690, 1984.
- [9] S. Nikolaidis, P. Lasota, G. Rossano, C. Martinez, T. Fuhlbrigge, and J. Shah, "Human-Robot Collaboration in Manufacturing: Quantitative Evaluation of Predictable, Convergent Joint Action," *IEEE International Symposium on Robotics*, pp. 1-6, 2013.
- [10] J. Mainprice and D. Berenson, "Human-Robot Collaborative Manipulation Planning Using Early Prediction of Human Motion," (in English), *2013 IEEE/RSJ International Conference on Intelligent Robots and Systems (IROS)*, pp. 299-306, 2013.
- [11] C. J. Hasson, T. Shen, and D. Sternad, "Energy Margins in Dynamic Object Manipulation," *Journal of Neurophysiology*, vol. 108, no. 5, pp. 1349-65, Sep 2012.
- [12] D. Sternad, "Human Control of Interactions with Objects - Variability, Stability and Predictability," (in English), *Geometric and Numerical Foundations of Movements*, vol. 117, pp. 301-335, 2017.
- [13] D. Sternad and C. J. Hasson, "Predictability and Robustness in the Manipulation of Dynamically Complex Objects," *Advances in Experimental Medicine and Biology*, vol. 957, pp. 55-77, 2016.
- [14] P. Maurice, N. Hogan, and D. Sternad, "Predictability, Force and (Anti-)Resonance in Complex Object Control," *Journal of Neurophysiology*, Apr 18 2018.
- [15] B. Nasseroleslami, C. J. Hasson, and D. Sternad, "Rhythmic Manipulation of Objects with Complex Dynamics: Predictability over Chaos," *PLoS Computational Biology*, vol. 10, no. 10, p. e1003900, Oct 2014.
- [16] S. Bazzi and D. Sternad, "Robustness in Human Manipulation of Dynamically Complex Objects through Control Contraction Metrics," *IEEE Robotics and Automation Letters*, pp. 1-1, 2020.
- [17] S. Bazzi, J. Ebert, N. Hogan, and D. Sternad, "Convergence and predictability in human control of dynamically complex objects," *Chaos: An Interdisciplinary Journal of Nonlinear Science*, vol. 28, no. 103103, 2018.
- [18] S. Bazzi, J. Ebert, N. Hogan, and D. Sternad, "Stability and predictability in dynamically complex physical interactions," *IEEE International Conference on Robotics and Automation (ICRA 2018), Brisbane, Australia*, May 21-25. 2018.
- [19] R. Q. van der Lind and P. Lammertse, "Hapticmaster—a generic force controlled robot for human interaction," *Industrial Robot: An International Journal*, vol. 30, no. 6, pp. 515-524, 2003.
- [20] R. Q. van der Linde, "HapticMaster – a Generic Force Controlled Robot for Human Interaction," *Industrial Robot: An International Journal*, vol. 30, no. 6, pp. 515-524, 2003.
- [21] F. A. Mussa-Ivaldi, N. Hogan, and E. Bizzi, "Neural, Mechanical, and Geometric Factors Subserving Arm Posture in Humans," *Journal of Neuroscience*, vol. 5, no. 10, pp. 2732-43, Oct 1985.
- [22] E. Burdet, R. Osu, D. W. Franklin, T. Yoshioka, T. E. Milner, and M. Kawato, "A Method for Measuring Endpoint Stiffness during Multi-Joint Arm Movements," *Journal of Biomechanics*, vol. 33, no. 12, pp. 1705-9, Dec 2000.
- [23] B. W. Silverman, "Density Estimation for Statistics and Data Analysis," *Chemical Rubber Company Press*, p. 176, 1986.